ChemComm

COMMUNICATION

View Article Online
View Journal | View Issue

Cite this: *Chem. Commun.*, 2022, **58**, 3823

Received 12th January 2022,
Accepted 21st February 2022

DOI: 10.1039/d2cc00220e

rsc.li/chemcomm

A highly durable graphene monolayer electrode under long-term hydrogen evolution cycling†

Michel Wehrhold, [a] Tilmann J. Neubert, [a] Tobias Grosser,[a] Martin Vondráček, [b] Jan Honolka [b] and Kannan Balasubramanian *[a]

Achieving long term stability of single graphene sheets towards repeated electrochemical hydrogen evolution reaction (HER) cycling has been challenging. Here, we show through appropriate electrode preparation that it is possible to obtain highly durable isolated graphene electrodes, which can survive several hundreds of HER cycles with virtually no damage to the sp^2-carbon framework and persistently good electron transfer characteristics.

Single sheets of 2D materials, such as graphene, in pristine or modified form are emerging as promising candidates for electrocatalysis. In its pristine form, several electrochemical reactions have been studied on graphene, such as the hydrogen evolution reaction (HER).[1–5] The sp^2-conjugated carbon network is a rather poor electrocatalyst for the HER, due to the unfavorable adsorption energy of solvated protons onto pristine graphene.[6] However, chemical modification of graphene sheets and hybrid structures composed of graphene sheets can reduce the overpotential for the HER.[7] Moreover, single graphene sheets supported on noble or non-noble metal layers were found to exhibit good HER activity, sometimes approaching that of the crystalline Pt(111) surface.[8,9] On the other hand, heteroatom doping of carbon nanosheets has been shown to deliver electrocatalytic properties, raising the hopes of metal-free carbonaceous catalysts.[10,11] It has also been theoretically proposed that introducing defects[12] or varying the doping level of graphene[6,9] may allow for improved hydrogen adsorption thereby enhancing the HER.

One of the fundamental challenges, for the widespread use of graphene as an electrocatalyst, concerns the maintenance of the durability of the electrode composed of just a single sheet of carbon atoms. It has been shown that the HER can be observed on as-prepared monolayer graphene on an insulating substrate such as Si/SiO_2.[2,3] However, already after three cycles, the sheet was found to break apart, due to large hydrogen bubbles emanating from the HER.[2] Even in few layer graphene, it was found that the integrity of the sp^2-carbon framework is compromised upon HER cycling.[2] When a graphene sheet is supported on a metal substrate (*e.g.* Pt, Au, Fe), the HER is enhanced. One mechanism that has been discussed in this context is the possibility of protons to penetrate through the graphene layer, either directly or through single point defects,[13,14] and subsequently be reduced at the underlying metal electrode. In this scenario, the formation of hydrogen bubbles below the graphene sheet may lead to delamination causing physical changes of the graphene sheet.[4,15] Hence, for graphene to be usable as a good candidate for electrocatalysis, it is important that the electrode is durable under continuous gas evolution. Also with an underlying metal surface, the introduction of structural defects on graphene has been proposed as a way to favor hydrogen evolution.[4] On single crystalline Pt(111) electrodes, graphene was found to be extremely stable even after performing a thousand cycles of HER.[5,9] It should be noted that in the last two cases, graphene was directly synthesized on the Pt(111) crystal, in contrast to other graphene monolayer electrodes, which are typically chemical vapor deposition (CVD)-grown and are subsequently transferred to a desired substrate.

In this work, we focus on single CVD-grown graphene sheets on an insulating SiO_2 substrate and show that we can indeed realize graphene electrodes that show a high stability towards the HER for numerous cycles in three different acid solutions: HCl, $HClO_4$ and H_2SO_4. Specifically, we use an optimized preparation strategy,[16,17] which involves metal-ion-free etching of the copper substrate followed by an annealing and electrochemical etching step[18] to prepare intact single layer graphene electrodes mostly free of trace metal impurities. A graphene sheet prepared in this manner is very stably held on the insulating SiO_2 substrate. Using this elaborate preparation strategy, we observe that the electrodes can easily withstand

[a] *School of Analytical Sciences Adlershof (SALSA), IRIS Adlershof & Department of Chemistry, Humboldt-Universität zu Berlin, Germany. E-mail: nano.anchem@hu-berlin.de*
[b] *Institute of Physics, Academy of Sciences of the Czech Republic, Na Slovance 2, Prague 18221, Czech Republic*

† Electronic supplementary information (ESI) available. See DOI: 10.1039/d2cc00220e

at least 1000 cycles of HER in $HClO_4$ without undergoing any structural damage. Through systematic characterization using optical microscopy, atomic force microscopy (AFM) and Raman spectroscopy, we show that the HER cycling does not increase the defect density in the sp^2-carbon framework. Most importantly, the layer is found to be intact without any cracks or holes. Furthermore, through electroanalysis, we show that the electron transfer characteristics to a classical redox probe remain unaffected even after prolonged HER cycling experiments.

Graphene monolayer electrodes were prepared according to a fabrication strategy that we have outlined in our previous works.[17] Specifically, we use polystyrene as a polymer support to coat commercially obtained graphene on copper foils. The copper is etched away in an acidified peroxide solution, followed by transfer of the polystyrene–graphene stack onto a heat-treated Si/SiO_2 substrate with pre-fabricated platinum contacts (see Methods in the ESI† for details). In order to avoid any trapped water below graphene[19] and to obtain a maximal conformal contact with the underlying substrate, the samples are annealed in a N_2 atmosphere at 600 °C. The platinum contacts are passivated with a resin in order to ensure that only the graphene sheet is in contact with the solution. Following this, we perform an electrochemical etching step[18] to get rid of trace metal impurities, which may parasitically catalyze the HER and may lead to unwanted damage of the graphene sheet.

The stability was evaluated by cycling the potential in 0.1 M $HClO_4$ to promote hydrogen evolution. Fig. 1a shows selected cyclic voltammograms (CVs) in perchloric acid obtained at a typical graphene electrode, at which 100 cycles were performed. Here the evolution of hydrogen can be inferred from the high current density at the extreme cathodic potentials. Our graphene monolayer electrodes show an overpotential for the HER in the range of −0.42 to −0.47 V (*vs.* NHE, Normal Hydrogen Electrode) at a current density of 0.1 mA cm^{-2}. This overpotential and the magnitude of the observed current density at −1 V *vs.* NHE are similar to what has been observed on graphene on copper electrodes.[3] The onset potential for the HER has been reported to be sensitive to substrate-induced doping of graphene. At these cathodic potentials, we also observe bubble formation (see Fig. S1 and the supporting video, ESI†). The magnitude of the current due to the HER and the onset potential show only little changes during the cycling. The slight cycle-to-cycle variation at high overpotential (< -0.8 V) is attributed to H_2 bubble formation on the electrode surface, which causes some noise in the current measurement. To examine the structural stability, atomic force microscopy (AFM) was carried out on the same electrode before and after performing the HER. Fig. 1b shows an AFM image of an electrode region before the HER. A height of <1 nm can be extracted for graphene from the line profiles, with a few wrinkles and cracks observable, which are typical for CVD-grown graphene on SiO_2. Fig. 1c displays an AFM image of the same position after the HER cycling, which shows that the graphene sheet remains completely intact after the 100 cycles of the HER. No additional cracks, holes or even roll-up of graphene was introduced by the cycling. We can see that the

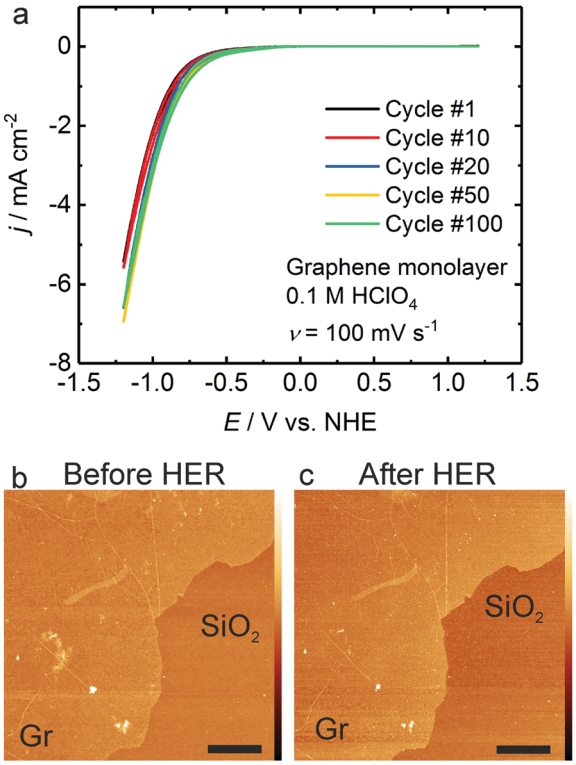

Fig. 1 (a) Cyclic voltammograms (selected cycles) measured in $HClO_4$ at a graphene electrode on Si/SiO_2 during a 100 cycle HER experiment. *j*: current density, *E*: applied potential. (b and c) AFM images of the region of the graphene (Gr) monolayer electrode before (b) and after (c) HER cycling. Lateral scale: 2 μm. Height scale: 20 nm.

graphene monolayer surface was even more clean after the HER cycling through the removal of some surface contamination. This is a tremendous improvement (see another example in Fig. S2 in the ESI†) in comparison to previous work showing that graphene was already destroyed after the first two cycles of the HER.[2] Similar performance was also observed at the fabricated graphene electrodes in HCl and H_2SO_4 solutions (see Fig. S3 in the ESI†).

To understand and determine the limits of stability (as inferred by an absence of morphological changes in the optical and AFM images) of our graphene monolayer electrodes, two series of experiments were carried out. In the first series, we wanted to test the maximum number of cycles of HER that graphene can withstand, while in the second series, we decided to test the limit of the extreme vertex potential to which graphene can be polarized without undergoing damage. In the first series, we found that graphene can easily withstand at least 1000 cycles of continuous HER cycling. Fig. 2a shows CVs measured at the first and 1000th cycle during such an experiment, while Fig. 2b presents a color map of the current measured during the entire HER cycling. It is quite clear that there is little change in the current density or onset potential during or after cycling. On this electrode, we have evaluated the integrity of the graphene sheet by measuring the electron transfer properties to a classical redox probe (ferrocenedimethanol – FDM). Fig. 2c presents CVs of FDM at this electrode before and after performing the 1000 cycles of HER.

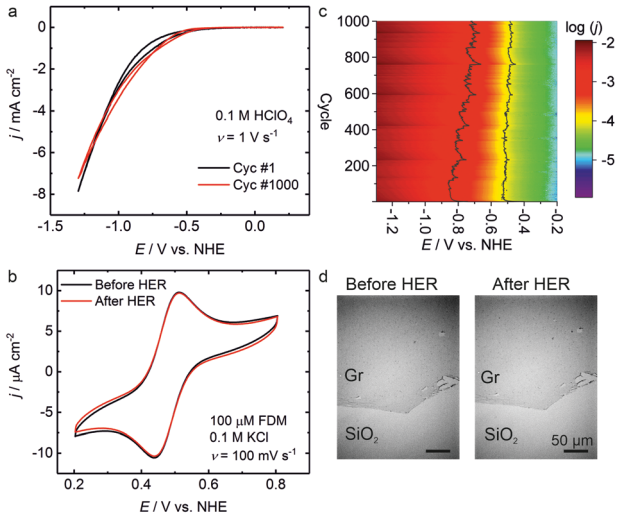

Fig. 2 (a) Comparison of the first (black) and last (red) CV cycles of a 1000 cycle HER experiment at graphene. (b) The current density (j, in A cm^{-2}) measured through the entire 1000 cycles is presented as a heat map (log scale). The lines in the map indicate contours of the constant current density of 0.1 mA cm^{-2} and 1 mA cm^{-2}. (c) Redox behavior of ferrocenedimethanol (FDM) measured by CV before (black) and after (red) the 1000 cycles of HER at the graphene electrode. (d) Optical images of the same area of the graphene (Gr) monolayer electrode before (left) and after (right) HER cycling.

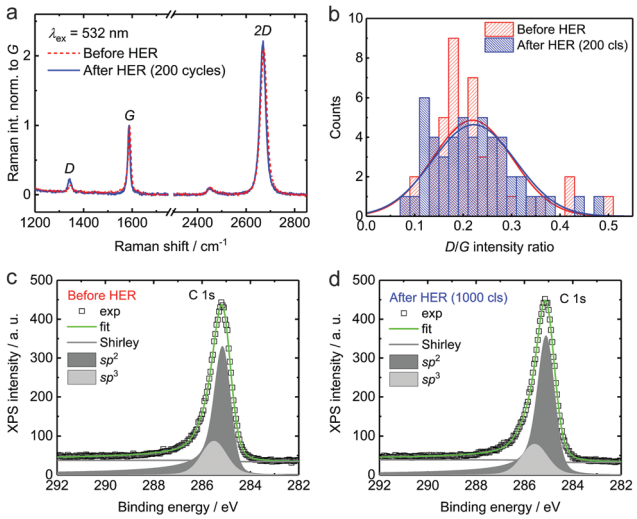

Fig. 3 (a) Representative Raman spectra from the same location of a graphene monolayer electrode before and after 200 cycles of HER. The spectra are normalized to the intensity of the G-peak. (b) Histogram of the ratio of D-to-G peak intensity extracted from Raman spectra measured at 50 different locations of a graphene electrode before and after 200 cycles of HER. Every solid curve is a fit to a normal distribution. (c and d) High-resolution carbon 1s XPS data before (c) and after (d) 1000 cycles of HER. Included are also fits corresponding to sp^2 and sp^3 fractions. See Fig. S9 in the ESI† for further details of XPS.

The magnitude of the current and the peak potentials are unaffected through the extensive HER cycling experiment. The structural integrity of the sheet is further attested by optical images (see Fig. 2d) obtained before and after the 1000 cycle-HER, where no new cracks, holes or folds are visible (see further examples in Fig. S4 in the ESI†). In the second series of experiments with varying vertex potential, we found that our electrodes survive cathodic potentials at least up to −1.5 V *vs.* NHE (in contrast to −1.3 V *vs.* NHE in previous works[2,3]) without any damage to the graphene sheet (see Fig. S5 and S6 in the ESI† and associated discussion). Overall, the data indicate that the graphene monolayer electrodes are surviving the excessive electrochemical HER cycling in $HClO_4$ as well as in HCl and H_2SO_4.

In order to obtain an idea of the efficiency of hydrogen evolution on graphene, we have performed a Tafel analysis of the data obtained through the CVs (see Fig. S7a in the ESI† for a complete profile of the Tafel slopes). We extract the Tafel slope in the range of 320–470 mV dec^{-1}, which indicates a rather sluggish and slow hydrogen evolution at our graphene monolayer electrodes compared to classical Pt electrodes or graphene supported on metals. This is not surprising since the adsorption of the protons onto pristine graphene has a very high energy barrier.[6] Our Tafel slope values are much higher than the values obtained at graphene on copper.[3] There, the underlying copper is expected to catalyze the HER on graphene through several possible mechanisms, such as a change in surface adsorption energy of protons or holes on graphene or permeability of graphene to protons.[4,6,9] In our case, we do not have any metal below graphene and hence we do not expect to have enhanced HER. Our values are also higher than previous reports[2,3] of graphene on SiO_2 by around 100 mV dec^{-1}. In contrast to the transfer method used there, we use a metal-ion free etching solution followed by an electrochemical etching step, which ensures that we have nearly no trace metal impurities in our samples. Such trace metal impurities could catalyze the HER,[18,20] if not removed properly, and may result in lower Tafel slopes. In fact, the values reported there are between our values and those for graphene on copper. Moreover, as in our previous work,[17] we ensure using X-ray photoemission spectroscopy (XPS) that we have a high proportion of sp^2-carbon in our samples (see Fig. 3). We have also extracted a measure of the exchange current density in our electrode (see Fig. S7b in ESI†), which lies in the range of 4–10 μA cm^{-2}. If we assume that the HER undergoes a mechanism similar to that on metals,[21] we can estimate a proton adsorption energy of around 45 kcal mol^{-1}, which is close to the theoretically estimated hydrogen adsorption energy for graphene.[6]

To gather further support for the high structural integrity of our graphene electrodes under the HER, we have carried out detailed Raman spectroscopic analysis and XPS on our electrodes before and after the electrochemical cycling measurements. Fig. 3a presents typical confocal Raman spectra obtained at a specific location in the device of Fig. 1 in its initial state and after 200 cycles of the electrochemical measurements. Raman peaks characteristic of monolayer graphene – D-, G- and 2D-peaks – are unambiguously identifiable in the spectra. We observe a strong 2D-peak approx. twice as high in intensity as the G-peak, which is typical for our as-prepared samples. The acquisition time was set high enough in these measurements to

accumulate enough counts in order to observe the D-peak with a sufficient resolution, since the relative intensity of this peak (I_D/I_G) gives us an idea about the defect density in the graphene sheet.[22] In order to obtain statistically significant information,[23] Raman spectra were collected as maps of 5 by 5 spots with a spacing of 5 μm at several locations before and after HER experiments. Parameters such as the relative intensities of the D- and 2D-peak (normalized to the G-peak) and the positions of the three peaks were extracted from such spectra. Fig. 3b presents a histogram of the observed I_D/I_G ratios before and after the HER cycling experiments. It can be inferred here that there is nearly no change in the mean ratio signifying a negligibly small change in the density of defects after the HER cycling experiments. Furthermore, the ratio of the 2D-to-G peak intensity and the positions of the D-, G- and 2D-bands are nearly unaffected (within the instrument resolution of ± 3 cm^{-1}) by the HER experiments (see Fig. S8 in ESI†). Fig. 3c shows high-resolution XPS data from the C1s region for a graphene electrode before HER cycling, where a single rather narrow peak is apparent, reflecting mainly sp^2 and some sp^3-carbon fraction. The peak position is shifted by around +0.7 eV from the theoretically expected value of 284.4 eV, since the XPS spectra were measured on an insulating substrate.[17] Fig. 3d shows a corresponding C1s spectrum after 1000 cycles of HER, with no significant changes in the position and composition of the carbon peak. This is quite remarkable considering that we have performed several 100 cycles of HER using the one-atom-thick electrode. The XPS survey spectra of the two samples are also similar (see Fig. S9 in the ESI† for further details of XPS).

In conclusion, we can say that careful preparation can indeed allow the repeated use of graphene electrodes for the HER on Si/SiO_2 substrates with ultrahigh chemical and mechanical stability. It is known in carbon research that the preparation of the electrode has a strong effect on the ensuing electrochemical characteristics.[17,24,25] This is in contrast to non-crystalline metal electrodes, which present similar electrochemical behavior rather independent of the preparation strategy. This work underlines the necessity to perform sample preparation carefully in order to assess the maximum achievable performance. It is worth mentioning that pristine graphene has also been found to be suitable for application as a potassium ion battery anode.[26] Starting out with such electrodes, through appropriate defect engineering[27] or chemical modification, we can reliably fabricate novel electrodes for the HER as well as for other electrocatalytic applications.

Funding from the German Science Foundation (DFG) *via* the Graduate School of Analytical Sciences Adlershof (GSC1013 SALSA) and *via* grant INST 276/754-1 is gratefully acknowledged. NanoESCA/XPS measurements were supported by the Czech Ministry of Education, Youth and Sports project SOLID21 CZ.02.1.01/0.0/0.0/16_019/0000760. We thank Stephan Schmid and Birgit Lemke from MPI Stuttgart for help with metal deposition and Gina-Maria Erler and Michael Winterfeld from HU Berlin and Martin Muske from HZB for assistance with sample fabrication.

Conflicts of interest

There are no conflicts to declare.

Notes and references

1 J. Li, Z. Zhao, Y. Ma and Y. Qu, *ChemCatChem*, 2017, **9**, 1554–1568.
2 A. García-Miranda Ferrari, D. A. C. Brownson and C. E. Banks, *Sci. Rep.*, 2019, **9**, 15961.
3 A. Xie, N. Xuan, K. Ba and Z. Sun, *ACS Appl. Mater. Interfaces*, 2017, **9**, 4643–4648.
4 A. J. Shih, N. Arulmozhi and M. T. M. Koper, *ACS Catal.*, 2021, **11**, 10892–10901.
5 Y. Fu, A. V. Rudnev, G. K. H. Wiberg and M. Arenz, *Angew. Chem., Int. Ed.*, 2017, **56**, 12883–12887.
6 E. Santos and W. Schmickler, *J. Phys.: Condens. Matter*, 2021, **33**, 504001.
7 B. Xia, Y. Yan, X. Wang and X. W. Lou, *Mater. Horiz.*, 2014, **1**, 379–399.
8 K. Hu, T. Ohto, Y. Nagata, M. Wakisaka, Y. Aoki, J.-I. Fujita and Y. Ito, *Nat. Commun.*, 2021, **12**, 203.
9 T. Kosmala, A. Baby, M. Lunardon, D. Perilli, H. Liu, C. Durante, C. Di Valentin, S. Agnoli and G. Granozzi, *Nat. Catal.*, 2021, **4**, 850–859.
10 K. Qu, Y. Zheng, X. Zhang, K. Davey, S. Dai and S. Z. Qiao, *ACS Nano*, 2017, **11**, 7293–7300.
11 Y. Zheng, Y. Jiao, L. H. Li, T. Xing, Y. Chen, M. Jaroniec and S. Z. Qiao, *ACS Nano*, 2014, **8**, 5290–5296.
12 H. Kawabata and H. Tachikawa, *Jpn. J. Appl. Phys.*, 2020, **59**, 025508.
13 J. L. Achtyl, R. R. Unocic, L. Xu, Y. Cai, M. Raju, W. Zhang, R. L. Sacci, I. V. Vlassiouk, P. F. Fulvio, P. Ganesh, D. J. Wesolowski, S. Dai, A. C. T. van Duin, M. Neurock and F. M. Geiger, *Nat. Commun.*, 2015, **6**, 6539.
14 Y. An, A. F. Oliveira, T. Brumme, A. Kuc and T. Heine, *Adv. Mater.*, 2020, **32**, 2002442.
15 S. Yasuda, K. Tamura, T.-O. Terasawa, M. Yano, H. Nakajima, T. Morimoto, T. Okazaki, R. Agari, Y. Takahashi, M. Kato, I. Yagi and H. Asaoka, *J. Phys. Chem. C*, 2020, **124**, 5300–5307.
16 T. J. Neubert, M. Wehrhold, N. S. Kaya and K. Balasubramanian, *Nanotechnology*, 2020, **31**, 405201.
17 M. Wehrhold, T. J. Neubert, A. Yadav, M. Vondráček, R. M. Iost, J. Honolka and K. Balasubramanian, *Nanoscale*, 2019, **11**, 14742–14756.
18 R. M. Iost, F. N. Crespilho, L. Zuccaro, H. K. Yu, A. M. Wodtke, K. Kern and K. Balasubramanian, *ChemElectroChem*, 2014, **1**, 2070–2074.
19 O. Ochedowski, B. K. Bussmann and M. Schleberger, *Sci. Rep.*, 2014, **4**, 6003.
20 L. J. A. Macedo, R. M. Iost, A. Hassan, K. Balasubramanian and F. N. Crespilho, *ChemElectroChem*, 2019, **6**, 31–59.
21 P. Quaino, F. Juarez, E. Santos and W. Schmickler, *Beilstein J. Nanotechnol.*, 2014, **5**, 846–854.
22 L. G. Cançado, A. Jorio, E. H. M. Ferreira, F. Stavale, C. A. Achete, R. B. Capaz, M. V. O. Moutinho, A. Lombardo, T. S. Kulmala and A. C. Ferrari, *Nano Lett.*, 2011, **11**, 3190–3196.
23 J. M. Englert, P. Vecera, K. C. Knirsch, R. A. Schäfer, F. Hauke and A. Hirsch, *ACS Nano*, 2013, **7**, 5472–5482.
24 P. R. Unwin, A. G. Güell and G. Zhang, *Acc. Chem. Res.*, 2016, **49**, 2041–2048.
25 A. Yadav, M. Wehrhold, T. J. Neubert, R. M. Iost and K. Balasubramanian, *ACS Appl. Nano Mater.*, 2020, **3**, 11725–11735.
26 D. Wu, B. Yang, H. Chen and E. Ruckenstein, *Adv. Sustainable Syst.*, 2020, **4**, 1900152.
27 S. Grewal, A. M. Andrade, Z. Liu, J. A. G. Torres, A. J. Nelson, A. Kulkarni, M. Bajdich and M. H. Lee, *Adv. Sustainable Syst.*, 2020, **4**, 2000048.

